A Transceiver Architecture for Ultrasonic OFDM with Adaptive Doppler Compensation

Tran MinhHai, Saotome Rie, Suzuki Taisuki
Graduate School of Engineering and Science
University of the Ryukyus
No.1 Senbaru, Nishihara, Okinawa, Japan
{haitran, saotome, suzuki}@lsi.ie.u-ryukyu.ac.jp

Tomohisa Wada
Department of Information Engineering
University of the Ryukyus
No1. Senbaru, Nishihara, Okinawa, Japan
wada@lsi.ie.u-ryukyu.ac.jp

***Abstract*—We propose an acoustic OFDM system for underwater wireless communication in vertical direction, between a mother ship in the surface and a robot at the sea bottom. In our experiments, the velocity changes roughly over time, though it is not very high. In addition, Doppler does not manifest itself explicitly in time compression/expansion, for example, a velocity of 1(m/s) causes a frequency offset of 16 (Hz), but a small compression/expansion of 1(sample/an OFDM symbol). Therefore, we propose an adaptive Doppler compensation consisting of two stages without resampling. The first stage is phase de-rotation to compensate a common frequency offset before FFT processing. The second stage is non-uniform Doppler compensation by an ICI matrix before channel estimation. To boost the range of frequency offset estimation, we use continual pilots in conjunction with monitoring the drifting of power delay profile over time. Experimental results taken in Shizuoka, Japan show our system using QPSK, and 16QAM achieved a data throughput of 7.5(Kbit/sec) with a transmitter moving at maximum 2(m/s), over 30m vertically.**

Keywords—OFDM, Expansion/Compression, Doppler, ICI

I. Introduction

To facilitate new industries and applications such as deep-sea mining, ocean discovering, sub-marine communication, and so on, Underwater Wireless Communication (UWC) is needed. In the last decades, several research groups have actively conducted experiments on UWC, and achieved impressive results. Acoustic OFDM has been considered a good solution for UWC, so far. Depending on target applications, several acoustic OFDM systems have been proposed [1-8], and those are considered state-of-the-art methods.

Systems in [3-6] used resampling technique to compensate the Doppler effect that is one of the greatest challenges in acoustic OFDM systems. However, applying the resampling based method is not suitable for our system. We aim to a vertical link communication between a robot at the sea bottom and a mother ship in the surface, in which, the maximum relative speed between a transmitter and receivers is about 2.5(m/s). The Doppler effect does not manifests itself explicitly in compression/expansion, but significantly in frequency offset in our system. So, it is not easy to estimate accurately the time compression/expansion over an OFDM symbol. In addition, when the velocity changes roughly over OFDM symbols such as during pulling/pushing a transmitter in our experiment, symbol-by-symbol Doppler compensation is needed. To do so, we track the Doppler shift over OFDM symbols by using continual pilots. Instead of resampling, we compensate the Doppler effect through two stages. The first stage is a common phase de-rotation performed before FFT, and the second stage is an ICI matrix performed before channel estimation. Simulation and experimental results showed our system yields a stable performance when the velocity change roughly over OFDM symbols.

The rest of this paper is organized as follow. Section II. shows signal model. Our proposed system is presented in Section III. Simulation and experimental results are shown in Section II. Finally, Section V is conclusion.

II. Signal Model

In this section, we model and figure out two impacts of Doppler effect in the frequency domain. The transmitted signal of an OFDM symbol can be written as

$$S(t) = Re\left\{\sum_{n=-N}^{N} C_n e^{j2\pi(f_c+f_0)t}\right\} \quad with\ 0 \le t \le T_0 \tag{1}$$

Totally, $(2N+1)$ subcarriers are utilized to carry information data. f_c and f_0 is carrier frequency and sub-carrier space, respectively. C_n denotes data carried by sub-carrier n. We assumed that there are L multipaths, each path has a gain of r_i, and a delay of τ_i. For our target application, that is, a vertical link communication between a robot in the sea bottom and a mother shift in the surface, all paths have a similar Doppler rate $\Delta(t)$. Thus, the received pass-band signal is written as follows

$$R_{PB}(t) = \sum_{i=0}^{L-1} r_i\, S\big(t(1+\Delta(t)) - \tau_i\big) \tag{2}$$

$$\Delta(t) = \frac{v(t)}{c}$$

In here, $v(t)$ is the relative moving speed between a transmitter and receivers. In the time domain,

978-0-933957-43-5 ©2015 MTS

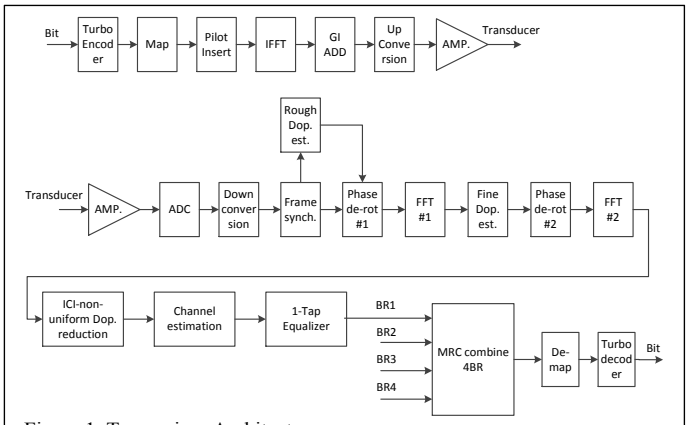

Figure 1. Transceiver Architecture

the Doppler effect manifests itself as sampling rate error, which is called time compression/expansion in [3-6]. A straightforward idea is re-sampling the distorted signal to compensate the Doppler effect. Different from those methods, we analyze and compensate impacts of the Doppler in frequency domain. After down-conversion, we get

$$R_{BB}(t) = \sum_{i=0}^{L-1} \sum_{n=-N}^{N} \left\{ A_i C_n e^{j2\pi n f_0 (1+\Delta(t))(t-\tau_i)} \right\} e^{j2\pi f_c \Delta(t) t} \tag{3}$$

$$A_i = r_i e^{-j2\pi f_c (1+\Delta(t))\tau_i} \tag{4}$$

First, all sub-carrier experiences a common frequency offset of $f_c\Delta(t)$(Hz). Second, each sub-carrier experiences a different frequency offset of $nf_0\Delta(t)(Hz)$, which depends on the position of a sub-carrier. This is called position-dependent frequency offset, or so-called non-uniform Doppler shift in [8]. The position-dependent frequency offset significantly degrades performance of high modulation such as 16 and 64QAM. In our case, a moving speed of $1(m/s)$ causes the common Doppler shift of $16(Hz)$ which is equal to $16(\%)$ of subcarrier space. In addition, the edge subcarriers corresponding to $n = \pm 40$ suffers a frequency offset of $\pm 2.5(Hz)$ which is equivalent to 2.5% of subcarrier space. The central subcarrier $n = 0$ does not experience this kind of frequency offset. Therefore, we must take position-dependent frequency offset into account.

III. Our Proposed System

A. Coarse time and frequency synchronization

Due to harsh conditions including high Doppler, long delay spread, ambient noise, and impulsive noise, we use a preamble consisting of 3 OFDM symbols for coarse time and frequency synchronization. Similar to [9], we use two identical symbol X_1 and X_2 to detect the starting point of a data frame. Two sliding windows are used to calculate the self-correlation between X_1 and X_2 at the receiver side.

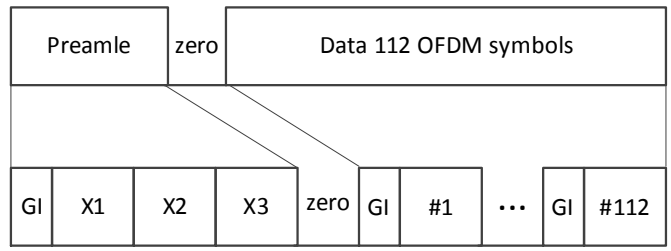

Figure 2. Data Frame Structure

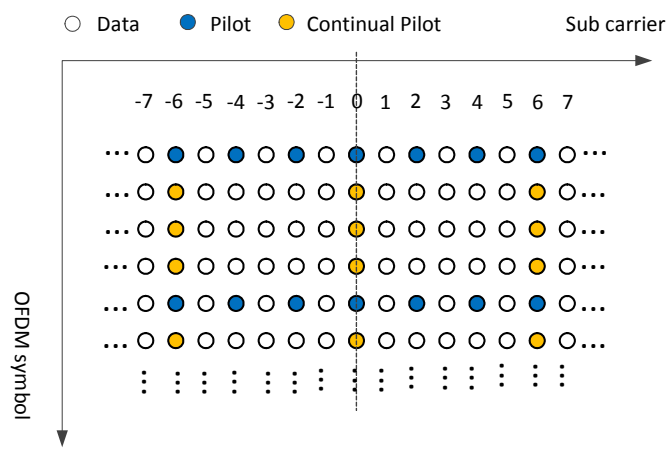

Figure 3. Continual Pilot

Table 1. System Parameter

Parameters	Value
TX-RX Elements	1 TX/4 RX Transducer
Sampling Frequency	96000 Hz
TX Center Frequency	24000 Hz
Band Width	8000 Hz
FFT Size	2048
OFDM symbol length T0	21.333 ms
GI length	0.5T0
Sub Carrier Spacing	46.875 Hz
Number of Sub Carrier	161

Next, Cyclic Prefix (CP) of the X_1 symbol is used to estimate the fraction part of frequency offset. Inspired from [10], we use symbol X_2 and X_3 to estimate the integer part of the frequency offset, which might up to few times of the sub-carrier space. We inserted data into all sub-carrier rather than only even sub-carrier as in [10]. In short, our idea is to perform a phase differential modulation using symbol X_2 and X_3 as follows

$$U(k) = X_2(k) X_3^*(k) \tag{5}$$

At the receivers, we get

$$V(k) = Y_2(k) Y_3^*(k) \tag{6}$$

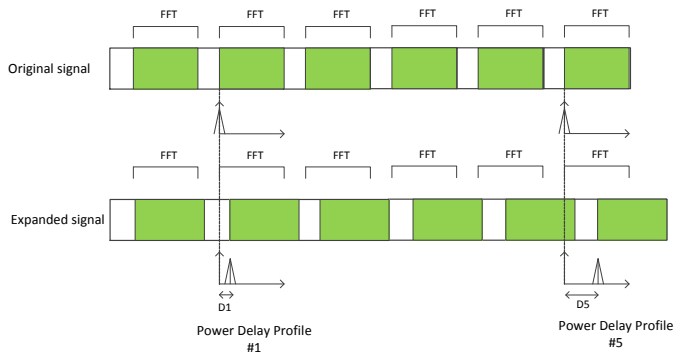

Figure 4. Power Delay Profile drifting due to compression/expansion

After compensating the fractional frequency offset, we calculate a metric as follow to estimate the integer frequency offset as follows

$$f_I = \arg\max_{f_I} \sum_{k=0}^{N} U(k)V^*(k + f_I) \tag{7}$$

B. Frequency offset tracking by using continual pilot combined monitoring the power delay profile

Using the continual pilot as in [11-12] is convenient for tracking frequency offset over time, however, the maximum frequency offset can be estimate is $\frac{f_0}{2(1+T_{GI})}$. To boost the range of frequency offset estimation, we monitor the drifting of power delay profile over time. In addition, the accuracy of frequency estimation by using continual pilots is worsen since continual pilots already corrupted by severe ICI. So, a rough estimation/compression frequency offset before using continual pilots is very helpful.

The continual pilot is inserted as shown Fig. 3. Briefly, the difference in phase between two successive pilots indicate the frequency offset as follow

$$H(m,n) = \frac{Y(m,n)}{X(m,n)}, m \in S_p \tag{8}$$

$$\hat{f}_F = \frac{1}{M} \sum_{m \in S_p} \frac{anlge\{H(m,n)^* H(m,n+1)\}}{2\pi(1 + T_{GI})} \tag{9}$$

In here, $H(m,n)$ is the channel transfer function estimated at sub-carrier m and symbol n, and T_{GI} is guard interval length.

Due to time compression/expansion caused by Doppler effect, the observed power delay profile (PDF) is drifted over time when a fixed FFT window is applied. This phenomenon is described in Fig. 4. The drift amount of PDF over time indicates time compression/expansion and corresponding frequency offset caused by Doppler effect.

$$\hat{f}_R = f_c \frac{D_1 - D_5}{4T_{sb}} \tag{10}$$

Here, T_{sb} is the OFDM symbol length included guard interval, and f_c is carrier frequency. After compensating the $\hat{f}_R$ by a simple phase de-rotation, the residual frequency offset is estimated by using continual pilots as mentioned above.

C. Adaptive Doppler Compensation

In this section, we show two stages to compensate the Doppler shift without resampling. We first perform a phase de-rotation to compensate the common frequency/phase rotation before FFT. Then, the received signal in (3) is written as

$$R_{BB}(t) = \sum_{n=-N}^{N} H_n C_n e^{j2\pi n f_0 (1+\Delta)t} \tag{11}$$

$$H_n = \sum_{i=0}^{L-1} r_i e^{-j2\pi(fc+nf_0)(1+\Delta)\tau_i} \tag{12}$$

After FFT demodulation, the received data at k^{th} subcarrier is

$$Y_k \approx H_k C_k e^{j\pi\Delta k} + \sum_{\substack{l=-N \\ l \neq k}}^{N} H_l C_l \left[\Delta\left(\frac{l}{l-k}\right) e^{j\pi\Delta l}\right] \tag{13}$$

$$I(k,l) = \begin{cases} e^{j\pi\Delta k} & if\ k = l \\ \Delta\left(\frac{l}{l-k}\right) e^{j\pi\Delta l} & if\ k \neq l \end{cases} \tag{14}$$

$I(k,l)$ represents Inter-carrier interference from subcarrier l to subcarrier k. It is noted that $I(k,l)$ not just depends on Doppler rate Δ, and distance $(l-k)$ between two subcarriers, but also depends on position of subcarrier l. In another word, edge sub-carriers suffer severe ICI than center subcarriers. So the second stage is compensating the position dependent frequency offset by an ICI matrix before channel estimation. The assumption that all delay paths have the same Doppler shift leads to an interesting result, that is impact of non-uniform Doppler shift and frequency selective fading is separable as shown in the below matrix equation.

Since the main diagonal of I is much greater than off-diagonals, and absolute values of $I(k,l)$ decay quickly when going far from the main diagonal, there are several ways to avoid finding an inverse of I such as Jacobi iteration method as in [13].

$$\begin{bmatrix} Y_{-N} \\ Y_{-N+1} \\ \vdots \\ Y_{N+1} \\ Y_N \end{bmatrix} = \begin{bmatrix} I_{-N,-N} & I_{-N,-N+1} & \cdots & I_{-N,N-1} & I_{-N,N} \\ I_{-N+1,-N} & I_{-N+1,-N+1} & \cdots & I_{-N+1,N-1} & I_{-N+1,N} \\ \vdots & \vdots & \ddots & \vdots & \vdots \\ I_{N-1,-N} & I_{N-1,-N+1} & \cdots & I_{N-1,N-1} & I_{N-1,N} \\ I_{N,-N} & I_{N,-N+1} & \cdots & I_{N,N-1} & I_{N,N} \end{bmatrix} \begin{bmatrix} H_{-N}D_{-N} \\ H_{-N+1}D_{-N+1} \\ \vdots \\ H_{N-1}D_{N-1} \\ H_N D_N \end{bmatrix} \quad (15)$$

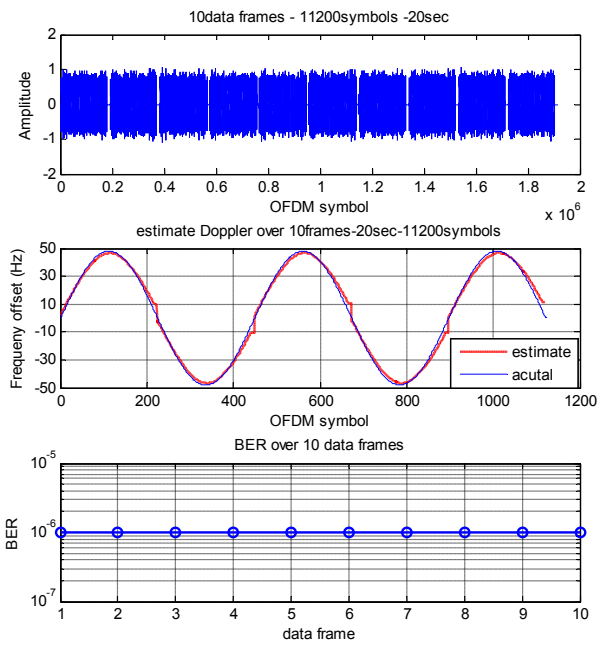

Figure 5. Simulation BER of QPSK over 10 frames/1120 symbols

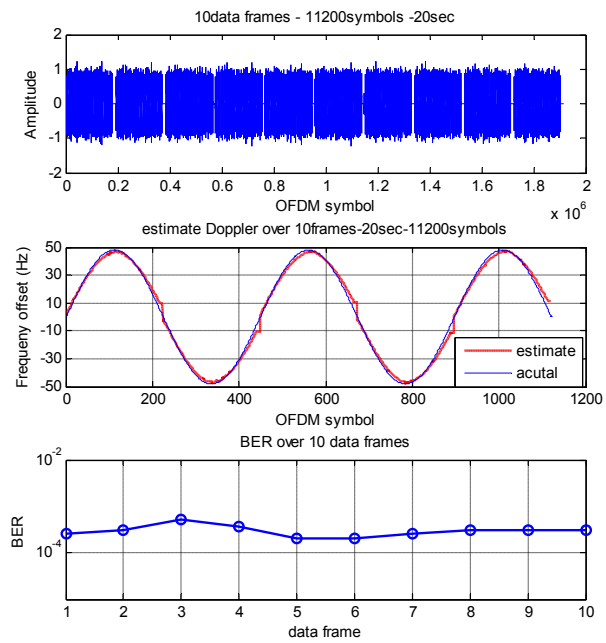

Figure 6. Simulation BER of 16QAM over 10 frames/1120 symbols

IV. Simulation and Experimental Results

Considering a communication in vertical direction, usually there are a direct path and a surface reflection path. In addition, when the transmitter moving, all paths has a similar Doppler rate. For simulation we use a channel with 3 paths as in Table II. Most importantly, our system aims to mitigate the changing roughly of velocity over time, such as during pulling/pushing the transmitter in our experiment. We create a simulation scenario, in which, the velocity changes over time as shown in Fig. 5, 6. The maximum velocity is 3(m/s) corresponding to a frequency offset of 48(Hz), and the acceleration rate is about 1.7(m/s/s). As shown in Fig. 5 and 6, the estimate frequency offset is very close to the actual frequency offset. All Bit Error Rate (BER) is before Turbo decoding. QPSK achieved free error, and 16QAM achieved a stable performance over 10 frames.

Our experiment setting is shown in Fig. 8. The transmitter was pull toward the surface, the push toward the bottom. When the transmitter approach near the surface, or the bottom its velocity gradually reduce, then changes direction, increase velocity again. So the velocity trajectory is quite complicate as shown in Fig. 9, 10 shows the estimation of the time varying Doppler shift over 6 frames. Our Doppler compensation provide a stable performance when the velocity changes over time. The BER in Fig. 9, 10 are before Turbo decoding, and it is free error after decoding. In addition, the estimated Delay Profile in Fig. 7 was consistent with the experiment setting. In the delay profile, there was a direct path, and a surface reflection path, and the distance between them is about $5(ms)$ which is equivalent to $7.5(m)$ distance. As the experiment setting, the receivers was in $3(m)$ depth which can lead to a surface reflection path of $7.5(m)$.

Table II. Multipath channel

Path	Delay(ms)	Gain (dB)
#1	0	0
#2	2(ms)	-5
#3	3(ms)	-7

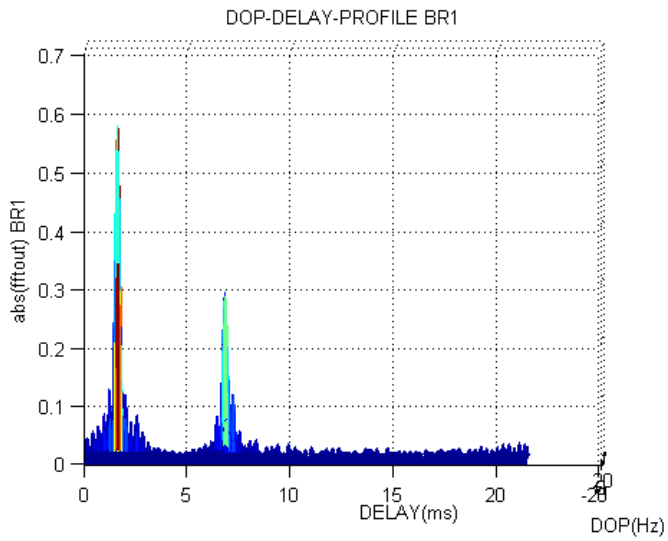

Figure 7. Channel Delay Profile Observed in Experiments

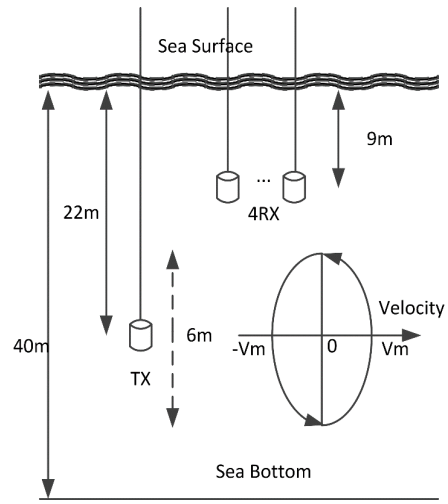

Figure 8. Experiment Setting

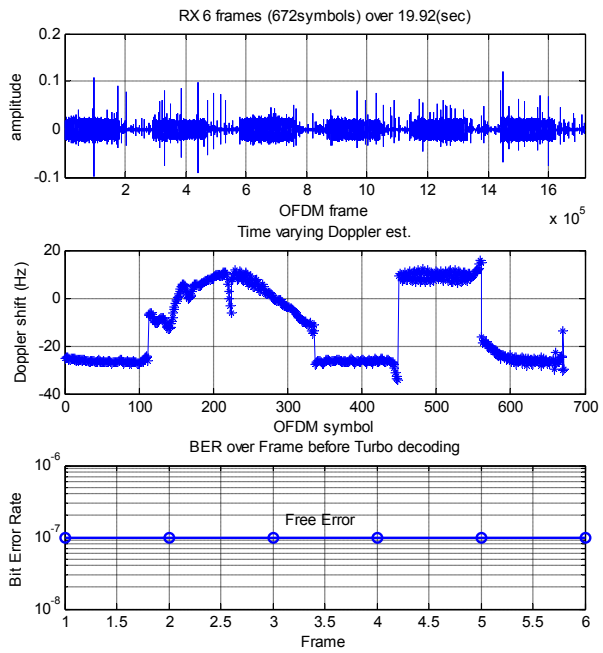

Figure 9. Experiment BER of QPSK over 6 frames/ 672 OFDM symbols

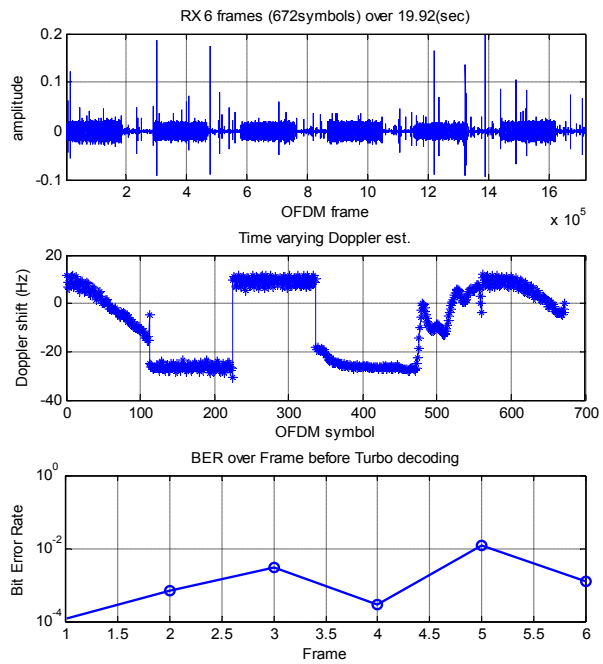

Figure 10. Experiment BER of 16QAM over 6 frames/ 672 OFDM symbols

V. Conclusion

In this paper, we presented an acoustic OFDM system with adaptive Doppler compensation. Instead of resampling, our proposal method compensates impacts of Doppler effect symbol-by-symbol by phase de-rotation and an ICI matrix. In addition, frequency offset is tracked over OFDM symbols by using continual pilot in conjunction with monitoring the drifting of the power delay profile. Simulation and experimental results confirmed that our system provided a stable performance when the velocity changes roughly over OFDM symbols.

Overall, we achieved a data throughput of 7.5 (kbit/sec) over more than 30(m) vertically, under a maximum speed of 2(m/s) between a transmitter and receivers, multipath channel, ambient noise, and impulsive noise. In addition, simulation results shows our system can work well under the maximum velocity of 3(m/s) while the velocity changes roughly over time.

REFERENCES

[1] Stojanovic, Milica. "Low complexity OFDM detector for underwater acoustic channels." *OCEANS 2006*. IEEE, 2006.

[2] Zorita, Eduard Valera, and Milica Stojanovic. "Space–Frequency Block Coding for Underwater Acoustic Communications." *Oceanic Engineering, IEEE Journal of* 40.2 (2015): 303-314.

[3] Li, B., Zhou, S., Stojanovic, M., Freitag, L., & Willett, P. (2008). Multicarrier communication over underwater acoustic channels with nonuniform Doppler shifts. *Oceanic Engineering, IEEE Journal of*, *33*(2), 198-209.

[4] Li, Baosheng, et al. "Non-uniform Doppler compensation for zero-padded OFDM over fast-varying underwater acoustic channels." *OCEANS 2007-Europe*. IEEE, 2007.

[5] Li, Baosheng, et al. "MIMO-OFDM for high-rate underwater acoustic communications." *Oceanic Engineering, IEEE Journal of* 34.4 (2009): 634-644.

[6] Abdelkareem, A. E., et al. "Low-complexity doppler compensation for OFDM-based underwater acoustic communication systems." *OCEANS, 2011 IEEE-Spain*. IEEE, 2011.

[7] Hai, Tran Minh, et al. "ULTRASONIC DIVERSITY OFDM TRANSCEIVER ARCHITECTURE WITH IMPULSIVE NOISE CANCELLING FOR SHALLOW SEA COMMUNICATION.", 2nd *Underwater Acoustics Conference and Exhibition UA2014*, June 22nd to 27th, 2014, Rhodes, Greece, page 1227-1232

[8] Suzuki, Takumi, Hai Minh Tran, and Tomotaka Wada. "An underwater acoustic OFDM communication system with shrimp (impulsive) noise cancelling."*Computing, Management and Telecommunications (ComManTel), 2014 International Conference on*. IEEE, 2014.

[9] Van de Beek, Jan-Jaap, Magnus Sandell, and Per Ola Borjesson. "ML estimation of time and frequency offset in OFDM systems." *IEEE transactions on signal processing* 45, no. 7 (1997): 1800-1805.

[10] Schmidl, Timothy M., and Donald C. Cox. "Robust frequency and timing synchronization for OFDM." *Communications, IEEE Transactions on* 45.12 (1997): 1613-1621

[11] Speth, Michael, Stefan A. Fechtel, Gunnar Fock, and Heinrich Meyr. "Optimum receiver design for wireless broad-band systems using OFDM. I."*Communications, IEEE Transactions on* 47, no. 11 (1999): 1668-1677.

[12] Speth, Michael, Stefan Fechtel, Gunnar Fock, and Heinrich Meyr. "Optimum receiver design for OFDM-based broadband transmission. II. A case study."*Communications, IEEE Transactions on* 49, no. 4 (2001): 571-578.

[13] Tran, Hai Minh, and Tomohisa Wada. "On ICI canceller for mobile OFDM DTV receivers." In *Advanced Communication Technology (ICACT), 2014 16th International Conference on*, pp. 290-297. IEEE, 2014.